ACS SyntheticBiology
Cite This: ACS Synth. Biol. 2019, 8, 1590−1600
Research Article
pubs.acs.org/synthbio

Reversing an Extracellular Electron Transfer Pathway for Electrode-Driven Acetoin Reduction

Nicholas M. Tefft[†] and Michaela A. TerAvest*[,†]

[†]Department of Biochemistry and Molecular Biology, Michigan State University, East Lansing, Michigan 48824, United States

Supporting Information

ABSTRACT: Microbial electrosynthesis is an emerging technology with the potential to simultaneously store renewably generated energy, fix carbon dioxide, and produce high-value organic compounds. However, limited understanding of the route of electrons into the cell remains an obstacle to developing a robust microbial electrosynthesis platform. To address this challenge, we leveraged the native extracellular electron transfer pathway in *Shewanella oneidensis* MR-1 to connect an extracellular electrode with an intracellular reduction reaction. The system uses native Mtr proteins to transfer electrons from an electrode to the inner membrane quinone pool. Subsequently, electrons are transferred from quinones to NAD^+ by native NADH dehydrogenases. This reverse functioning of NADH dehydrogenases is thermodynamically unfavorable; therefore, we added a light-driven proton pump (proteorhodopsin) to generate proton-motive force to drive this activity. Finally, we use reduction of acetoin to 2,3-butanediol via a heterologous butanediol dehydrogenase (Bdh) as an electron sink. Bdh is an NADH-dependent enzyme; therefore, observation of acetoin reduction supports our hypothesis that cathodic electrons are transferred to intracellular NAD^+. Multiple lines of evidence indicate proper functioning of the engineered electrosynthesis system: electron flux from the cathode is influenced by both light and acetoin availability, and 2,3-butanediol production is highest when both light and a poised electrode are present. Using a hydrogenase-deficient *S. oneidensis* background strain resulted in a stronger correlation between electron transfer and 2,3-butanediol production, suggesting that hydrogen production is an off-target electron sink in the wild-type background. This system represents a promising step toward a genetically engineered microbial electrosynthesis platform and will enable a new focus on synthesis of specific compounds using electrical energy.

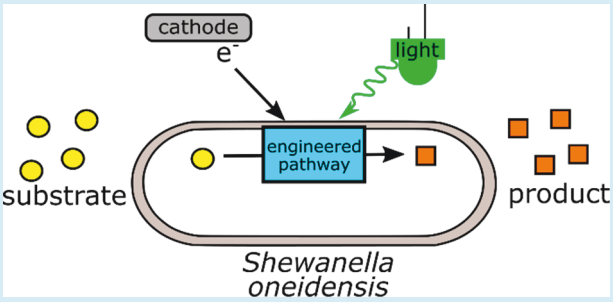

KEYWORDS: *Shewanella oneidensis, electrosynthesis, bioelectrochemical systems, proteorhodopsin*

Microbial electrosynthesis is a technology that utilizes microbes for production of useful chemicals using carbon dioxide, water, and electricity as feedstocks.[1] While most microbial electrosynthesis efforts to date have targeted fuel production, other possible applications include production of platform chemicals or bioplastics.[2] With pressure to develop sustainable production systems, microbial electrosynthesis is an attractive technology to simultaneously produce valuable products and store electricity generated by wind and solar technologies. Initial efforts have focused on three primary platforms for microbial electrosynthesis: pure cultures of acetogens,[3,4] undefined mixed cultures,[5,6] and electron shuttles paired with model bacterial strains.[7,8] While these approaches have demonstrated proof-of-concept, significant improvements in product yield and product spectrum are necessary to make microbial electrosynthesis economically viable.

Pure culture microbial electrosynthesis systems have been developed in an effort to understand the mechanism of electron uptake from a cathode. These systems primarily utilize acetogenic bacteria because they are naturally capable of converting carbon dioxide into acetate using hydrogen or other inorganic electron donors.[9,10] Multiple reports show that acetogens are capable of using an electrode in place of native electron donors.[3,4] While acetate is a relatively low value product, genetic modification may yield strains capable of producing other compounds through electrosynthesis.[11] While this is a promising approach, significant challenges to acetogen engineering remain, and further developments are necessary.[11,12] An alternative approach that may yield specific products is to utilize chemical electron mediators to transfer electrons from an electrode into existing model organisms. This approach has been successful in multiple organisms to generate products such as succinate and ethanol.[7,13−15] However, the cost of the mediator and downstream separations likely make this approach too costly for industrial scale-up. Similarly, biohybrid devices utilizing solid metal catalysts to promote electron transfer have shown promise in fuel production[16] and nitrogen fixation[17] but involve costly materials that may be difficult to scale up.

Mixed culture approaches to microbial electrosynthesis have also borne success due to their ability to generate a range of

Received: November 26, 2018
Published: June 7, 2019

DOI: 10.1021/acssynbio.8b00498
ACS Synth. Biol. 2019, 8, 1590−1600

products without genetic modification. Early efforts in this area have primarily generated acetate with adjustments to operating conditions driving increased yield.[18−20] However, other molecules can also be produced, including butyrate, butanol, and ethanol.[5,21] Selective enrichment of the community is important to improve yields and product specificity.[6,19] While evidence that higher value products are attainable increases the attractiveness of electrosynthesis using undefined mixed cultures, off-target production remains problematic. For example, increased abundance of methanogens over time has posed difficulties for long-term experiments due to decreased acetate titers and increased methane production.[6,22] Further, a mixed community cannot be engineered to produce a specific high-value compound with any current technology.

Overall, optimization of existing approaches to microbial electrosynthesis has been hampered by poorly defined interactions between bacteria and cathode electrodes. In most cases, the mechanism of electron transfer is unknown, although in mixed culture systems, H_2 is recognized as a major electron carrier between the electrode and microbes.[5] For pure cultures, direct electron transfer has been proposed but not proven.[3,4] Similarly, specific mechanisms of electron transfer via chemical mediators are only beginning to be investigated.[13] In contrast, transmembrane electron transfer is much better understood between dissimilatory metal reducing bacteria and anode electrodes.

Shewanella oneidensis MR-1 is a particularly well understood model organism for extracellular electron transfer and utilizes the Mtr pathway for transferring electrons to the outer surface of the cell (Figure 1).[23−30] The route of electron transfer between the electrode and cellular metabolism begins with CymA, an inner membrane tetraheme cytochrome *c* that acts as a hub to transfer electrons from the quinol pool to several terminal oxidoreductases.[28] From CymA, electrons can be transferred to periplasmic electron carriers (PEC), including FccA and CctA, which transfer electrons to MtrA.[31−33] Electrons then cross the outer membrane via the Mtr electron conduit, which is composed of MtrC, MtrA, and MtrB.[34] MtrC and MtrA are decaheme cytochromes responsible for transferring electrons across the outer membrane. The interaction between MtrA and MtrC is stabilized by a β-barrel, MtrB, which spans the outer membrane. Together, the CymA−MtrCAB system creates a pathway that connects the quinone pool in the inner membrane to electrode-exposed hemes at the outer surface of the cell. This pathway has mostly been studied in the context of its native activity: to transfer electrons from organic carbon oxidation to solid terminal electron acceptors such as metal oxides and anode electrodes.

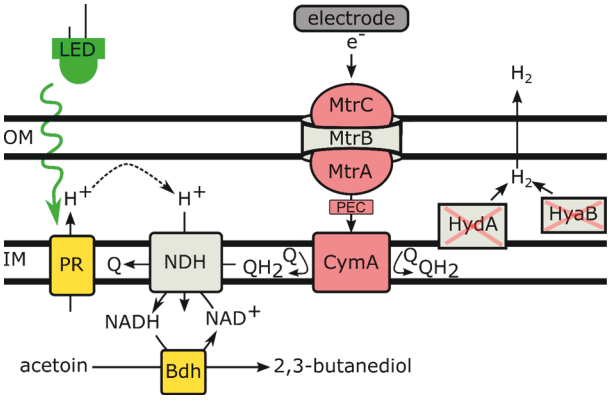

Figure 1. Engineered inward electron transfer pathway. *Shewanella oneidensis* MR-1 pathway designed to transfer electrons from the electrode to NAD^+ to generate intracellular reducing equivalents. Native proteins are shown in gray, or in the case of cytochromes, red. Heterologous proteins are shown in yellow. PEC: periplasmic electron carriers (FccA, CctA); OM: outer membrane; IM: inner membrane; LED: green light source. Function of hydrogenases HydA and HyaB was removed by deleting genes encoding these proteins to prevent generation of H_2, which acts as an electron sink under experimental conditions. This is indicated by a red X overlaid on each protein.

Existing knowledge of the Mtr pathway makes *Shewanella* an excellent candidate for engineering a microbial electrosynthesis system from the ground up using synthetic biology tools. Initial steps to explore the use of *S. oneidensis* MR-1 for microbial electrosynthesis have demonstrated reverse electron transfer through the Mtr pathway. Ross et al.[35] showed electron transfer from a cathode to *S. oneidensis* MR-1 with fumarate as an electron sink, indicating that the Mtr pathway can function in reverse to transfer electrons from a cathode to respiratory quinones. More recent work by Rowe et al.[36] has demonstrated that *S. oneidensis* MR-1 can also catalyze electron transfer from a cathode to oxygen through the Mtr pathway and the quinone pool.

While previous work has demonstrated the ability to generate reduced quinones via a cathode, this is not sufficient to power intracellular reduction reactions. Electrons in the quinone pool have too positive a redox potential to be spontaneously transferred to NAD^+ (ca. −80 mV_{SHE} for menaquinone:menaquinol vs ca. −320 mV for NAD^+:NADH) and have only been transferred to electron acceptors with a more positive redox potential, such as fumarate (ca. + 30 mV_{SHE}). Electrons should ideally be transferred to an intracellular, lower potential electron carrier to be useful for electrosynthesis. NADH is a promising intracellular electron carrier to target because it is involved in many metabolic reactions and is relatively accessible from the quinone pool through NADH dehydrogenases. Under typical conditions, NADH dehydrogenases catalyze the favorable transfer of electrons from NADH to quinones and conserve energy as a proton-motive force.[37] However, NADH dehydrogenases may also catalyze the reverse redox reaction, utilizing proton-motive force as an energy source, as observed in purple photosynthetic bacteria.[38]

On the basis of previous work and our knowledge of *S. oneidensis* MR-1 metabolism, we hypothesized that NADH dehydrogenases could be driven in reverse to transfer electrode-derived electrons into the cell. Therefore, we sought to catalyze intracellular reductions by relying on the native Mtr pathway and NADH dehydrogenases for electron transfer steps and using a heterologous light-driven proton pump, proteorhodopsin (PR), to generate proton motive force (PMF) to drive NADH dehydrogenases in reverse (Figure 1). PMF generation is necessary because electron transfer from reduced quinones to NAD^+ is thermodynamically unfavorable ($\Delta_rG'^\circ$ = +48.6 kJ/mol for menaquinone). Because NADH dehydrogenases couple NADH oxidation to proton pumping to generate PMF, we hypothesized that the same complexes could catalyze the reverse process and couple PMF dissipation to NAD^+ reduction. Indeed, this reverse function of NADH dehydrogenases has previously been observed in *Rhodobacter* spp.[39] Using PR allowed us to generate PMF to drive NADH dehydrogenases in reverse without relying on native metabolic

DOI: 10.1021/acssynbio.8b00498
ACS Synth. Biol. 2019, 8, 1590−1600

Table 1. Strains and Plasmids Used in This Study

strain or plasmid	description	source
E. coli		
Mach1	host strain for plasmids	
WM3064	conjugation strain for *S. oneidensis*	
S. oneidensis		
MR-1	wild type	63
Δ*hyaB*Δ*hydA*	hydrogenase double knockout mutant	43, 45, 64
plasmids		
pBBR1-MCS2	kan resistance, broad host vector	65
pBBR1-PR	pBBR1MCS2 bearing proteorhodopsin (uncultured marine gamma proteobacterium EBAC31A08)	41, 66
pBdh	pBBR1MCS2 bearing butanediol dehydrogenase gene from *Enterobacter cloacae*	this study
pBdh-PR	pBBR1MCS2 bearing butanediol dehydrogenase from *Enterobacter cloacae* and proteorhodopsin (uncultured marine gamma proteobacterium EBAC31A08)	this study

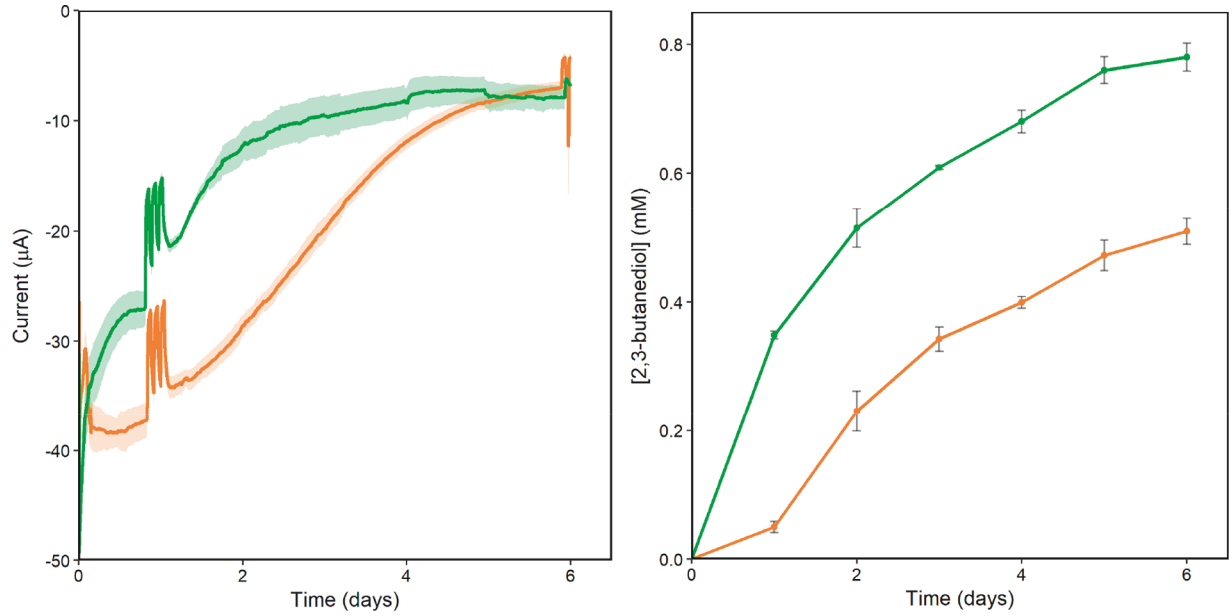

Figure 2. Removal of native hydrogenases decreases current and increases 2,3-butanediol production. (A) Current and (B) 2,3-butanediol accumulation observed in bioreactors containing cells expressing Bdh and holo-PR. The strain without hydrogenases is shown in dark green, and the wild-type background is shown in orange. Data shown were measured beginning at injection of 10 mM acetoin (time 0). Each point represents the average of three replicates with standard error shown in transparent ribbons or error bars. Changes in current at ∼1 day are when lights were cycled off and on at 1 h intervals to verify function of holo-PR.

processes that could potentially confound our experimental results. We also expressed butanediol dehydrogenase (Bdh) and provided its substrate, acetoin, to provide an electron sink and a mechanism to track NADH generation. This system represents a generalizable platform to use cathodes to drive NADH-dependent reductions in *S. oneidensis* MR-1. Further development of this platform could lead to a new capability to generate specific, high-value compounds using electricity and carbon dioxide as feedstocks.

RESULTS AND DISCUSSION

Development of Modified *S. oneidensis* Strains. Genes encoding PR and Bdh were cloned into a medium copy plasmid (Figure S1) and conjugated into *S. oneidensis* (both wild-type and a strain lacking hydrogenases; Δ*hyaB*Δ*hydA*) (Table 1). The plasmid expressed both genes in a synthetic operon from a *lac* promoter, which is constitutive in *S. oneidensis* MR-1 due to the absence of a native *lac* repressor. Transcription termination of both genes was controlled by the same rho-independent terminator already present on the pBBR1MCS2 plasmid. Ribosome binding site sequences were optimized for maximum strength in *S. oneidensis* using the Salis RBS calculator.[40] A FLAG tag was added to the C-terminus of each protein to facilitate detection by Western blot. Both proteins were detectable in cleared lysates using an anti-FLAG antibody, confirming successful expression (Figure S2). To confirm function of Bdh, the modified strain was grown aerobically in the presence of 15 mM exogenous acetoin in LB. Accumulation of 2,3-butanediol was observed by HPLC, indicating that the expressed Bdh is functional (Figure S3). Function of PR expressed from a similar plasmid was previously demonstrated in *S. oneidensis* MR-1.[41,42]

Cathodic Current Drives Acetoin Reduction and Hydrogen Production. To determine the capability of the engineered cells to accept electrons from a cathode, strains carrying a plasmid with PR and Bdh were pregrown and inoculated into bioelectrochemical systems at a final density of OD_{600} = 0.17. The working electrode was poised at a cathodic potential of −0.03 V_{SHE}; N_2 sparging was used to remove oxygen from the system, and acetoin was added to a final

DOI: 10.1021/acssynbio.8b00498
ACS Synth. Biol. 2019, 8, 1590−1600

Table 2. Charge Balance Summary of Presented Experiments

hyaB hydA	−0.3 V_{SHE}	holo-PR	Bdh	anodic start	mol e^-	2,3-butanediol exp (mM)	2,3-butanediol obs (mM)	Figure
+	+	−	+	−	0.10 ± 0.01	0.29 ± 0.03	0.33 ± 0.05	2
+	+	+	+	−	0.11 ± 0.01	0.33 ± 0.01	0.51 ± 0.02	2
−	+	−	+	−	0.05 ± 0.00	0.15 ± 0.00	0.4 ± 0.03	2
−	+	+	+	−	0.07 ± 0.01	0.21 ± 0.02	0.8 ± 0.02	2
−	+	−	+	+	0.04 ± 0.0	0.12 ± 0.01	0.16 ± 0.01	5
−	+	+	+	+	0.06 ± 0.01	0.17 ± 0.02	0.19 ± 0.01	5
−	−	−	+	+			0.08 ± 0.01	5
−	−	+	+	+			0.13 ± 0.01	5
−	+	−	−	+	0.04 ± 0.01	0.12 ± 0.02		6
−	+	+	−	+	0.05 ± 0.00	0.14 ± 0.00		6

concentration of 10 mM. Each bioelectrochemical system was equipped with green LED lights around the working electrode chamber to drive proton pumping by PR (Figure S4). A common question in previous work on microbial electrosynthesis is whether H_2 mediates electron transfer. To address this, we initially compared performance of strains with wild-type or hydrogenase mutant backgrounds. We used a hydrogenase knockout strain previously developed by Marshall et al.[43] that does not have the ability to use molecular hydrogen as an electron source or sink.[44−46]

To determine whether a hydrogen mediated pathway would function when hydrogenases were present, we compared electron uptake and 2,3-butanediol production between strains in either background. We observed that overall current was lower in the hydrogenase mutant background than the wild-type background, while 2,3-butanediol accumulation showed the opposite trend (Figure 2; note that for cathodic current, a greater negative current represents a greater amount of electron transfer). This indicates that rather than acting as a mediator, H_2 was an electron sink for *S. oneidensis* on the cathode. If hydrogen acted as a mediator in this system, we would expect a simultaneous decrease in both current and 2,3-butanediol when hydrogenases were absent. Our results indicate that cells with hydrogenases generated H_2 and that when the pathway to hydrogen was cut off, electrons were directed more efficiently toward acetoin reduction.

We calculated the amount of 2,3-butanediol accumulation expected based on total charge transfer over the course of the experiment and found accumulation was 0.59 mM higher than expected in the hydrogenase mutant background (Table 2). We predicted the extra 2,3-butanediol accumulation occurred due to oxidation of residual organic carbon in the system. This effect was exacerbated in the hydrogenase mutant strain, suggesting that hydrogen was an electron sink for both electrode-derived and organic-carbon-derived reducing equivalents. To reduce the effect, we modified the experimental protocol and performed all further experiments with the hydrogenase mutant strain.

Light and Current Drive a Target Reduction Reaction in Modified *S. oneidensis*. Because we observed significantly more 2,3-butanediol production than expected based on charge transfer (Table 2), we modified the procedure to reduce the influence of contaminating organic carbon as an electron donor. We modified the procedure so that the bioelectrochemical systems initially contained oxygen (ambient), and the working electrode was set at an anodic potential (+0.4 V_{SHE}). After 6 h, the working electrode was switched to a cathodic potential (−0.3 V_{SHE}), and N_2 sparging was used to remove oxygen from the bioreactors. After the working electrode was switched to a cathodic potential, a brief spike in cathodic current occurred, which dissipated in <2 h as oxygen was sparged out of the system (data not shown). After this period, a stable cathodic current between −5 and −8 μA was observed. After 16 h, an anoxic acetoin solution was injected into each bioreactor to a final concentration of 10 mM. After acetoin injection, an increase of −12 to −18 μA was observed in all bioelectrochemical systems (Figure 3).

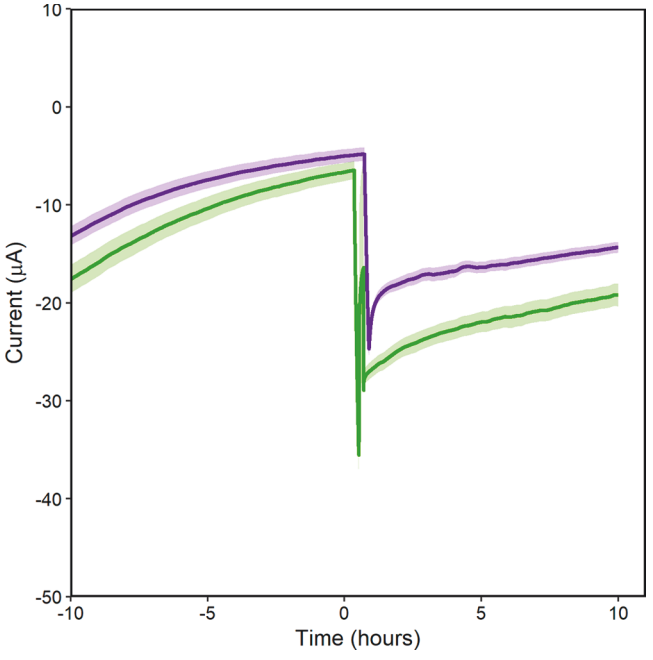

Figure 3. Cathodic current measurement during electron acceptor injection. Cathodic current increases significantly after the electron acceptor, acetoin, is added to the bioelectrochemical system. Time 0 represents 10 mM acetoin injection. Current measured in bioelectrochemical systems containing cells grown with holo-PR are shown in green, and those containing apo-PR are shown in purple. Each line represents the average of three replicates with standard error shown in transparent ribbons.

To determine the influence of proton pumping on electron uptake, we compared cells with and without functional PR by pregrowing the strain with or without the essential PR cofactor, all-*trans*-retinal. We refer to PR with retinal as holo-PR and PR without retinal as apo-PR. Cathodic current was significantly higher (p = 0.03) in systems with holo-PR (Figure 4). We confirmed that the increased current was due to PR activity by turning off the LED lights attached to the bioreactor. When the lights were turned off, cathodic current generated by cells with

DOI: 10.1021/acssynbio.8b00498
ACS Synth. Biol. 2019, 8, 1590−1600

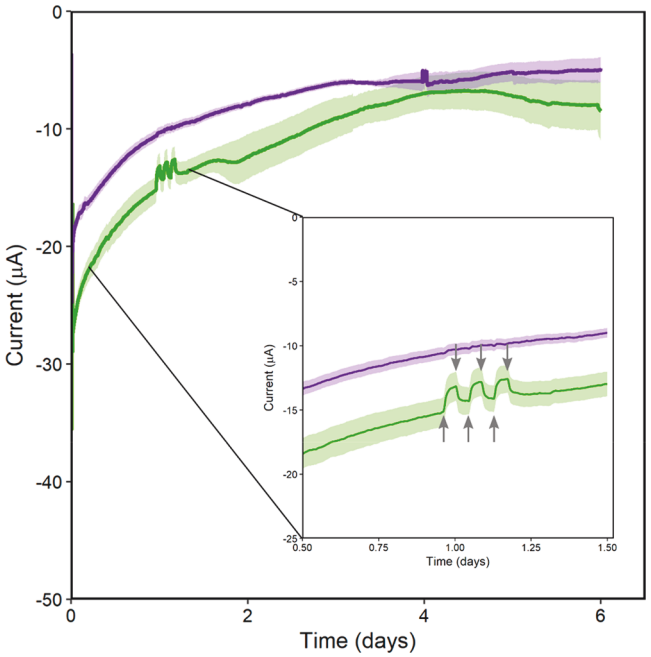

Figure 4. Response of cathodic current to green light. Current was measured in bioelectrochemical systems with electrodes poised at −0.3 V_{SHE}. Current shown was measured beginning at injection of 10 mM acetoin (time 0). Current measured in reactors containing cells with holo-PR is shown in green, and that measured in reactors containing apo-PR is shown in purple. Inset graph shows current change due to removal or addition of green light. Lights were turned off for 3 1 h intervals beginning just before time = 1 day. Each line represents the average of three replicates with standard error shown in transparent ribbons.

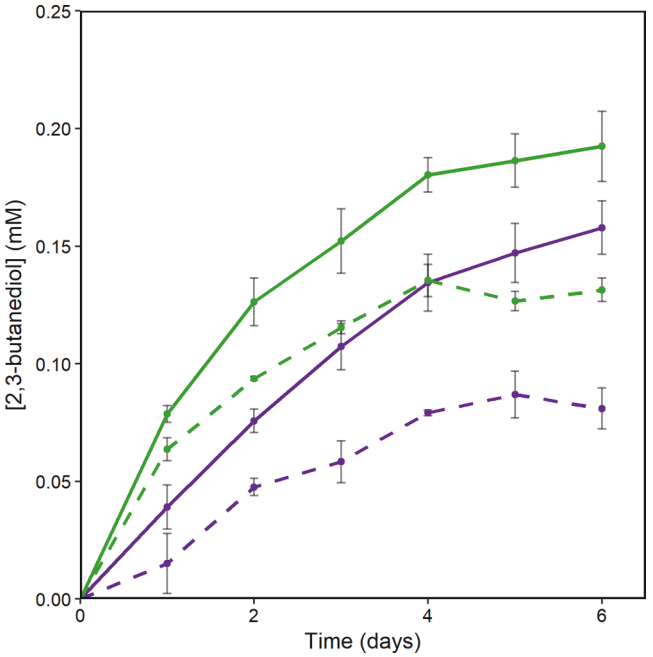

Figure 5. 2,3-Butanediol accumulation increases when potential is applied to the working electrode. HPLC measurement of 2,3-butanediol concentration in bioelectrochemical systems over time. Samples taken from working electrode chambers with electrodes poised at −0.3 V_{SHE} are shown in solid green and purple lines. Samples taken from bioelectrochemical systems disconnected from the potentiostat are shown in dashed green and purple lines. Samples from reactors containing cells with holo-PR are shown in green, and those containing apo-PR are shown in purple. Each point represents the average of three replicates with standard error shown in error bars.

holo-PR decreased, while cells with apo-PR were unaffected (Figure 4). This supports the model that the effect of light is dependent on functional PR; if the effect of light was due to heating or interaction of light with native components, we would expect cells with apo-PR to have a similar response to cells with holo-PR. The dependence of current on holo-PR and light supports our hypothesis that enhanced PMF generation by PR promotes electron uptake by the modified strain.

During the same experiment, we also measured 2,3-butanediol accumulation to determine whether cathodic electrons were directed toward the target reaction, acetoin reduction. As with current, 2,3-butanediol accumulation was greater in the bioelectrochemical systems with holo-PR (Figure 5). Based on the total charge transfer over the course of 6 days, accumulation of 0.17 ± 0.02 mM 2,3-butanediol was expected by the end of the experiment (Table 2). Accumulation of 0.19 ± 0.01 mM 2,3-butanediol was actually observed. The experiment was repeated using the same conditions with the exception that the electrode was disconnected from the potentiostat. This experiment confirmed that a portion of acetoin reduction was driven by the electrode (Figure 5). 2,3-Butanediol production was significantly reduced when the electrode was not poised (p = 0.01), and accumulation of only 0.13 ± 0.01 mM was observed. Based on our observations, 0.06 mM of the 2,3-butanediol (32% of total production) was generated through the electrode-dependent process. We hypothesize that 2,3-butanediol was not completely eliminated when the electrode was not poised because remaining organic carbon from the inoculum could be oxidized to generate the NADH needed for acetoin reduction. Although we attempted to remove as much organic carbon from the experiment as possible, some cells may have lysed during the washing and inoculation process, thus providing organics to the surviving cells.

To investigate the influence of organic carbon further, we also looked for evidence of lactate and acetate by HPLC. Lactate was used as a carbon source in precultures and could potentially be carried over into the bioelectrochemical systems, and acetate is a metabolic byproduct of anaerobic *S. oneidensis* metabolism.[47] A peak corresponding to lactate was not detectable in any samples from the bioelectrochemical systems. Acetate could only be analyzed in samples taken before acetoin injection because acetate elutes at the same time as acetoin in our HPLC method. However, we did not observe a peak corresponding to acetate in any sample taken between inoculation and acetoin injection. This suggests that organic carbon influencing acetoin reduction is likely coming from cell biomass rather than substrate carryover.

It was surprising that either holo-PR or the poised electrode alone increased 2,3-butanediol production. For cells with the unpoised electrode, the increase caused by holo-PR alone could be caused by increased viability. As observed previously,[41] we saw that cells with holo-PR maintained a higher cell density over the course of the experiment than cells with apo-PR, although it should be noted this difference was not statistically significant (Figure S5). Cells with holo-PR may have also had an increased ability to scavenge organic carbon in the bioelectrochemical system through increased availability of PMF to power transport.[41] The increase in 2,3-butanediol production caused by the electrode alone is more difficult to

DOI: 10.1021/acssynbio.8b00498
ACS Synth. Biol. 2019, 8, 1590−1600

explain. To make the redox reaction favorable when it is not coupled to PMF dissipation, the menaquinone pool would have to be in a highly reduced state (10 000 menaquinol per menaquinone) and the NAD(H) pool in a highly oxidized state (10 000 NAD^+ per NADH). These values fall outside the physiological ranges by orders of magnitude (e.g., a typical NAD^+:NADH value is 10:1), making this explanation seem unlikely. Another possible explanation is that there is an unknown source of PMF generation in *S. oneidensis* MR-1 in the culture conditions used here. Overall, further work is necessary to fully characterize the influence of PMF on inward electron transfer.

To determine whether acetoin reduction (as an electron sink) was necessary for inward electron transfer, we also performed experiments with strains lacking *bdh*. These experiments were performed using a very similar plasmid previously generated by Johnson et al.[41] When Bdh was not expressed, no 2,3-butanediol was detectable in the bioreactors after 6 days, and cathodic current was significantly reduced ($p = 0.02$). The strain without Bdh generated ca. −11 μA when holo-PR was present (Figure 6), representing a ca. 32% reduction in electron transfer compared to the strain with Bdh. This indicates that full activity of the inward electron transfer system is dependent on acetoin reduction, although there is also some Bdh-independent electron transfer. This experiment also allows us to refine our comparisons between charge transfer and 2,3-butanediol accumulation. By subtracting the total charge transfer catalyzed by the strain without Bdh from the strain with Bdh, we can calculate the amount of charge transfer that is Bdh-dependent (Table 2). We calculate that 0.03 mM of 2,3-butanediol accumulation is expected based on the amount of Bdh-dependent electron transfer. This amount of charge transfer agrees well with the 0.06 mM of electrode-dependent 2,3-butanediol accumulation that we observed. Electron uptake by the strain without Bdh was light-dependent when holo-PR was present, suggesting that the Bdh-independent process requires PMF generation. This may indicate that the Bdh-independent process also relies on reverse activity of NADH dehydrogenases, although we do not yet know the eventual fate of electrons transferred to the cells without Bdh.

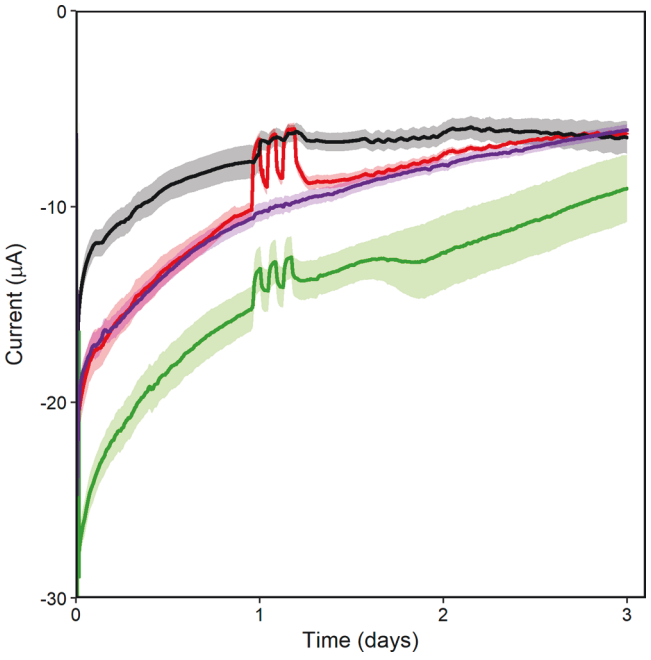

Figure 6. Both proteorhodopsin and butanediol dehydrogenase increase current. Current measured in bioelectrochemical systems containing cells expressing Bdh-PR with holo-PR is shown in green, and that measured in bioelectrochemical systems containing apo-PR is shown in purple. Current measured in reactors containing cells expressing only holo-PR is shown in red, and that measured in reactors containing only apo-PR is shown in black. Current was measured in bioreactors with electrodes poised at −0.3 V_{SHE}. Current shown begins at injection of 10 mM acetoin (time 0). Each line represents the average of three replicates with standard error shown in transparent ribbons. Changes in current at ∼1 day are when lights were cycled off and on at 1 h intervals to verify function of holo-PR

Evaluation of Cell Density and Total Protein in Bioelectrochemical Systems. To evaluate the possible effects of holo-PR on cell viability and lysis,[41] optical density in the bioelectrochemical systems was monitored during the experiments (Figure S5). We did not observe growth of the cells under any tested condition. Cells with holo-PR maintained a slightly higher OD_{600} over time compared to cells with apo-PR, although the difference was not statistically significant. Cell density was not significantly different between experiments with poised or unpoised electrodes. Because many cells were associated with the electrode surface and were not observed in cell density measurements, we also measured total protein in the bioelectrochemical systems at the end of the experiments (Figure S6). Total protein amounts were similar in all conditions. Overall, there were no obvious relationships between cell density or total protein and electron uptake and 2,3-butanediol production rates.

Comparison with Previous Work. Our results represent an advance in the field of microbial electrosynthesis because we have demonstrated a pathway to generate intracellular reducing power with a detailed understanding of the electron transfer mechanism. The transmembrane electron conduit connecting the quinol pool to electrodes has been very well characterized[23−25,30,48] and is known to be reversible.[35,49] We hypothesized that we could take inward electron transfer in *S. oneidensis* MR-1 one step further by utilizing PMF to overcome the thermodynamic barrier of the quinol:NAD^+ reduction and an excess of electron sink (Bdh/acetoin) to avoid over-reduction of the NAD^+:NADH pool. The results presented here support that hypothesis; we have shown that electron transfer to the target reaction is dependent on the electrode and on each of the modifications made to the strain. Further, the target reaction is NADH-dependent, suggesting that we have connected the electrode to the intracellular NADH pool.

Ongoing and Future Work. While the system described here is one of the best understood inward electron transfer demonstrations to date, there is still more to learn. One critical knowledge gap is exactly how electrons are transferred from the quinol pool to NADH. The *S. oneidensis* MR-1 genome encodes four NADH:quinone oxidoreductases, and any of them could be involved in inward electron transfer.[37,50] Initial work with single knockout mutants has not yielded significant deviation from the wild-type background, likely because the four NADH dehydrogenases have overlapping functions.[50] Although we hypothesize that a double knockout strain that is defective in aerobic growth (Δ*nuoN*Δ*nqrF1*) would show reductions in inward electron transfer, we have not yet been able to grow the strain in minimal medium. In preliminary experiments, we observed that it was essential to preculture

DOI: 10.1021/acssynbio.8b00498
ACS Synth. Biol. 2019, 8, 1590−1600

strains in minimal medium; therefore, we have not yet been able to test the inward electron transfer ability of the double knockout strain. With additional optimization, studies with multiple NADH deletion strains will enable us to elucidate the link between respiratory quinones and NADH in our system.

It is important to note that excess riboflavin (1 μM) was added in these experiments. The Mtr pathway is necessary for flavin reduction by *S. oneidensis* MR-1; therefore, this addition is not likely to cause Mtr-independent electron transfer but rather will increase electron transfer rate between Mtr and the electrode.[24] Flavin mononucleotide (FMN) is secreted by wild-type *S. oneidensis* and partially hydrolyzed to riboflavin, resulting in up to micromolar flavin concentrations.[51,52] These flavins are essential for both outward[52,53] and inward[54] electron transfer via the Mtr pathway. We hypothesized that native riboflavin production would be limiting because of the lack of an organic carbon substrate in the bioelectrochemical systems. However, more recent experiments suggest that exogenous riboflavin addition may not be necessary (unpublished data). Indeed, it appears that the decrease in the electron transfer rate over time may have been caused by generation of radicals and other reactive species via flavin photochemistry.[55] Further work is currently underway to establish the link between riboflavin concentration, electron transfer, and acetoin reduction.

Performance of the inward electron transfer system would also likely benefit from significant optimization. For example, the bioelectrochemical systems utilized here were not ideal for quantifying and optimizing the influence of light, although we did observe some relationship between light intensity and electron uptake rate (data not shown). In the future, we plan to move to an experimental setup with a more controlled light delivery system. Further, expression levels of PR and Bdh were not optimized in this study. Performance can likely be enhanced by tuning protein levels.

In this study, we have successfully driven a heterologous reduction reaction inside living bacteria using an extracellular electrode as the electron source. Rather than using native capabilities of acetogenic bacteria, we engineered a metal-reducing organism to reverse the flow of electrons in its respiratory chain. This represents a proof of concept for inward electron transfer, and with further development can be used to upgrade bioproducts through electrofermentation or to fix CO_2. Because electrical energy is one of the inputs to the system, the organic molecules produced also represent storage of electrical energy. This type of storage strategy will become essential as wind and solar power capacity increase. Wind and solar energy are intermittent sources; therefore, robust energy storage methods are critical. While significant improvements in engineered microbial electrosynthesis must still be made, a critical mass of researchers forming around this concept will help propel *Shewanella*-based electrosynthesis toward real world application.

METHODS

Bacterial Strains, Plasmids, and Growth Conditions. Strains and plasmids used in this study are listed in Table 1. *E. coli* strains were grown at 37 °C with shaking at 250 rpm, and *S. oneidensis* strains were grown at 30 °C with shaking at 275 rpm. Strains were grown in lysogeny broth (Miller, Accumedia) for assembly and initial verification of strains. Strains bearing pBBR1-MCS2-derived plasmids were grown with a final concentration of 50 μg/mL kanamycin. Precultures for bioelectrochemical experiments were grown in M5 minimal medium: 1.29 mM K_2HPO_4, 1.65 mM KH_2PO_4, 7.87 mM NaCl, 1.70 mM NH_4SO_4, 475 μM $MgSO_4{\cdot}7H_2O$, 10 mM HEPES, 0.01% (w/v) casamino acids, 1× Wolfe's mineral solution ($AlK(SO_4)_2{\cdot}12\ H_2O$ was not included), and 1× Wolfe's vitamin solution (riboflavin was not included); pH adjusted to 7.2 with 5 M NaOH.[50] M5 medium was supplemented with D,L-lactate to a final concentration of 20 mM. M5 medium with the following modifications was used in the working electrode chamber during bioelectrochemical experiments: 100 mM HEPES, no carbon source, no casamino acids, 1 μM riboflavin.

Design and Assembly of Bdh and Bdh-PR Plasmids. We utilized a PCR-independent assembly method to generate constructs to express Bdh and PR in *S. oneidensis* MR-1. The gene sequence encoding butanediol dehydrogenase in *Enterobacter cloacae* was downloaded from the NCBI gene database (NCBI Reference NC_014121.1). The codon usage was optimized for *S. oneidensis* MR-1 using JCAT Codon Adaptation Tool (www.jcat.de). A FLAG tag[56] was added immediately before the stop codon and the Salis lab RBS calculator[40] was used to design an optimized RBS for the Bdh-FLAG sequence. Sequences of 20 base pairs flanking the target *Sma*I restriction sites in the pBBR1-MCS2 sequence were added as flanking regions on the codon optimized RBS-Bdh-FLAG sequence for use in assembly. The entire sequence was submitted to Integrated DNA Technologies for synthesis as a gBlock gene fragment. The same general procedure was utilized to add the gene coding for proteorhodopsin to the plasmid containing *bdh*. Transcription of *bdh* and PR was controlled by the same constitutive lac promoter and terminator (Figure S1).

We isolated pBBR1-MCS2 plasmid DNA from *E. coli* using an E.Z.N.A plasmid DNA kit (Omega Bio-Tek). Prepared plasmid DNA was linearized using *Sma*I (New England Biolabs) digestion for 4 h at 25 °C. The synthesized RBS-Bdh-FLAG insert was resuspended in water to a final concentration of 10 ng/μL and was assembled with linearized pBBR1-MCS2 plasmid using NEBuilder High Fidelity DNA assembly kit (New England Biolabs) using 50 ng of pBBR1-MCS2 and 100 ng of RBS-Bdh-FLAG insert. Assembled pBBR1-MCS2-Bdh was transformed into *E. coli* Mach1 chemically competent cells (Invitrogen). pBBR1-MCS2-Bdh-PR was prepared as above except pBBR1MCS2-Bdh was digested using NdeI and SpeI (New England Biolabs) for 3 h at 37 °C prior to assembly with the synthesized PR gene. Transformants were initially screened via PCR using M13 forward and reverse primers and then sequenced (Sanger sequencing, RTSF Genomics Core, Michigan State University) to verify proper assembly and transformation. Verified Bdh and Bdh-PR plasmids were transformed into chemically competent *E. coli* WM3064 for use in conjugation with *S. oneidensis* (Figure S7). Conjugation was performed using a standard protocol for *S. oneidensis* MR-1[57] with both wild type and the hydrogenase knockout mutant.[44,45]

Verifying Expression by Western Blot. Expression of Bdh and PR was verified via Western blot through use of FLAG tags added during gene synthesis. Cells were cultured in 5 mL of LB for 16 h before 200 μL was centrifuged for 2 min at 10 000 rpm. Supernatant was removed, and cells were resuspended in 200 μL of a mixture of 1 mL Laemmli buffer, 20 μL of concentrated bromophenol blue (JT Baker, D29303) in 5× Laemmli buffer, and 10 μL of 1 M DTT. Cells were

DOI: 10.1021/acssynbio.8b00498
ACS Synth. Biol. 2019, 8, 1590−1600

vortexed to mix and incubated at 95 °C for 10 min. A mini-PROTEAN tetra cell electrophoresis chamber (Biorad, 1658005EDU) was loaded with 1× TGS buffer. Samples were vortexed a 5 μL was loaded onto a mini-protean TGX stain free gel (Biorad, 4568095) alongside 5 μL of Precision Plus ladder (Biorad, 1610376).

Samples were run at 100 V for 1.5 h until dye front moved off the gel. The gel cassette was broken, and gel was removed to 1× Transfer buffer (Biorad, 10026938). Proteins were then transferred to a nitrocellulose membrane (Biorad, 1704270) using a Biorad Turbo transfer system (Biorad, 1704150). The membrane was rinsed with 30 mL TBST buffer; this buffer was discarded, and the membrane was blocked using 50 mL of 3% BSA TBST buffer for 1 h on an orbital shaker. Blocking solution was discarded and replaced with 30 mL of 3% BSA TBST buffer, and then 7.8 μL of 3.85 mg/mL anti-FLAG antibody (Sigma-Aldrich, F3165) was added. The membrane was then incubated for 16 h at 4 °C on an orbital shaker.

The membrane was then rinsed for 5 min with TBST buffer three times. After rinsing, 30 mL of 3% BSA TBST buffer with 0.0625 μL of antimouse antibody (Sigma-Aldrich, A9044) was added. The membrane was incubated for 1 h at RT. Buffer was discarded and the membrane rinsed with TBST buffer for 5 min, three times. ECL Clarity chemiluminescence solution (Biorad, 1705061) was prepared by mixing 10 mL of peroxide solution with 10 mL of enhancer solution and then adding the entire volume to the membrane. The membrane was incubated for 5 min; the ECL solution was discarded, and the membrane was imaged using a Kodak 4000R image station and Caresteam Molecular Imaging software.

Bioelectrochemical System Construction and Operation. Bioelectrochemical measurements were performed in custom two-chambered bioreactors separated by a cation exchange membrane (Membranes International, CMI-7000S) cut in a 4.5 cm circle to completely cover the 15 mm opening connecting working and counter chambers. Working electrodes were prepared from carbon felt (Alfa Aesar, 43200RF) cut into 50 × 25 mm rectangles and adhered to a titanium wire using carbon adhesive (Sigma-Aldrich, 09929-30G) and allowed to dry for 16 h. Although cells in the interior of the electrode are not exposed to light, we chose this electrode material because its surface roughness provides a large area for cells to colonize with access to both light and the electrode. Reference electrodes were prepared by oxidizing silver wires electrochemically in a dilute KCl solution and fixing them in saturated KCl-agar in a custom-made glass housing. The housing maintained ionic connection between the reference electrode and working chamber via a magnesia frit (Sigma-Aldrich, 31408-1EA). Counter electrodes were graphite rods 1/8″ in diameter (Electron Microscopy Science, 07200) suspended in the counter chamber filled with PBS. Working chambers were filled with 140 mL of M5 medium (100 mM HEPES, no Casamino acids) prior to autoclaving. After autoclaving, 1.7 mL 100× vitamin stock, 1.7 mL Wolfe's minerals (no $AlKSO_4H_2O$), 0.17 mL 50 mg/mL kanamycin, and 0.85 mL 0.2 mM riboflavin were added to the working chamber.

Reactors were connected to a potentiostat (VMP, BioLogic USA), and the working electrode was poised at +0.4 V_{SHE}. Current was measured every 1 s for the duration of the experiment. Current measurements were collected for at least 16 h prior to inoculation. Reactors were inoculated with cultures grown in 50 mL M5 medium supplemented with 20 mM D,L-lactate. Cultures were grown in 250 mL flasks at 30 °C for 17 h shaking at 275 rpm. After 17 h, 25 μL of 20 mM all-*trans*-retinal (vitamin A aldehyde, Sigma-Aldrich, R2500), the essential proteorhodopsin cofactor,[58] was added to designated flasks for functional PR testing to a final concentration of 10 μM, and all flasks were returned to incubator with shaking for 1 h.

To achieve higher inoculum density without adjusting growth time and phase, two 50 mL culture volumes were prepared for each reactor. Absorbance at 600 nm was determined for each culture using a biophotomer (Eppendorf, D30) before the volume was transferred to a 50 mL conical tube (VWR, 89039-664) and centrifuged for 5 min at 10 000 rpm (Thermo Scientific ST8R; Rotor: 75005709). Supernatant was removed, and a second volume of cells was added to the conical tube containing the cell pellet before a second centrifugation step. Supernatant was removed, and the combined pellets were resuspended in 10 mL of M5 (100 mM HEPES).

Absorbance at 600 nm was determined for each prepared volume of cells before being standardized to OD_{600} = 3.6. The working chamber of each bioelectrochemical system was then inoculated with 9 mL of standardized cell suspension using an 18g needle (Beckton Dickson, 305196) and 10 mL syringe (Beckton Dickson, 302995). The working electrode was poised at +0.4 V_{SHE} for 6 h in the presence of ambient oxygen before the potential was changed to −0.3 V_{SHE}, and N_2 gas, 99.9% (Airgas), was bubbled into the reactors through a 0.2 μm filter. The rate of flow of nitrogen gas was observed using a bubbler attached to the gas outlet line from the reactors. The rate of gas flow was maintained so there was positive pressure against the water in the bubbler and bubble rate was kept constant between reactors. After 16 h, sterile anoxic acetoin solution was added to a final concentration of 10 mM.

Prior to inoculation, 0.93 m of green LED light strips (FAVOLCANO, 600 LEDs/5 m, 24 W/5 m, ≤6 A/5 m) were attached to the exterior of the working chamber and switched on. This resulted in a photon flux of ∼250 μmol/s/m^2 at a typical experimental cell density of OD_{600} = 0.066. Photon flux was measured using a LI-250A light meter (LI-COR Biosciences) in a bioreactor set up to mirror typical conditions with the probe set adjacent to the surface of the electrode with green LED lights turned on. Light cycling was performed at 24 h post acetoin injection, lights were turned off for 1 h followed by 1 h on. Light cycles at 24 h were repeated three times, after which lights were left on.

Samples were regularly removed from the bioreactors for determination of OD_{600} and HPLC analysis. A 2 mL sample was taken approximately every 24 h using a 21g needle (Beckton Dickson, 305167) and 3 mL syringe (Beckton Dickson, 309657). One milliliter was used for determination of OD_{600}. One milliliter was transferred to a microcentrifuge tube (VWR, 20170-038) and frozen at −20 °C until preparation for HPLC analysis. Experiments without a set potential on the working electrode were set up as above except, immediately after acetoin injection, the potentiostat was disconnected from the working electrodes.

Experiments testing for the effect of hydrogenase activity (Figure 2) were performed as above except as follows. Potential was set to −0.3 V_{SHE} during background data collection, and no anodic potential was used. Oxygen removal using N_2 gas was also started during background data collection and continued for the entire experiment. Cultures

DOI: 10.1021/acssynbio.8b00498
ACS Synth. Biol. 2019, 8, 1590−1600

grown for reactor inoculation were standardized to the lowest observed OD_{600} after 18 h of growth instead of a target OD of 3.6. Finally, acetoin was injected 2 h after inoculation once a stable baseline current was achieved.

HPLC Analysis. HPLC analysis was performed on a Shimadzu 20A HPLC, using an Aminex HPX-87H (BioRad, Hercules, CA) column with a Microguard Cation H^+ guard column (BioRad, Hercules, CA) at 65 °C. Compounds of interest were separated using a 0.6 mL/min flow rate, in 5 mM sulfuric acid with a 30 min run time. Eluent was prepared by diluting a 50% HPLC-grade sulfuric acid solution (Fluka) in Milli-Q water and degassing the solution at 37 °C for 3−5 days before use. Compounds of interest were detected by a refractive index detector (Shimadzu, RID-20A) maintained at 60 °C. Samples were prepared by centrifuging 1 mL samples taken from the working electrode chambers for 10 min at 13,000 rpm in a microcentrifuge (Minispin Plus, Eppendorf) to remove cells. The supernatant was removed and transferred to a 2.0 mL glass HPLC vial (Vial: Restek, 21140; Cap: JG Finneran, 5395F09). Mixed standards of 2,3-butanediol and acetoin were prepared at concentrations of 1, 2, 5, 10, and 15 mM. Samples were maintained at 10 °C by an autosampler (Shimadzu, SIL-20AHT) throughout analysis. Acetoin and 2,3-butanediol concentrations in the samples were determined using linear calibration curves based on the external standards.

Expected 2,3-Butanediol Production Based on Charge Transfer. To determine maximum 2,3-butanediol production based on measured current values, the integral was determined for measured current beginning at 0 h (acetoin injection) and ending at 144 h. Current vs time curves were integrated numerically using R. This generated a mA·h value for each experimental condition. These values were then converted to expected 2,3-butanediol concentration (M) using the following equation.

$$\mathrm{mol/L} = \frac{\mathrm{mC{\cdot}h}}{\mathrm{s}} \cdot \frac{3600\ \mathrm{s}}{1\ \mathrm{h}} \cdot \frac{1\ \mathrm{C}}{1000\ \mathrm{mC}} \cdot \frac{6.24 \times 10^{18}\mathrm{e}^-}{1\ \mathrm{C}} \cdot \frac{1\ \mathrm{mol\ e}^-}{6.02 \times 10^{23}\mathrm{e}^-} \cdot \frac{1\ \mathrm{mol\ acetoin}}{2\ \mathrm{mol\ e}^-} \cdot \frac{1}{0.17\ \mathrm{L}}$$

Total Protein Analysis. Immediately upon cessation of each experiment, working electrodes were removed from the working chamber and placed in a 50 mL conical tube. The electrodes were frozen at −20 °C until preparation for determining total protein. A 2 mL sample of the remaining volume in the reactor was then taken; 1 mL was used for measuring absorbance at OD_{600}, and the second was frozen at −20 °C for later use in determining total protein. Electrode samples were prepared for total protein analysis by suspending harvested electrodes in 20 mL of 0.2 M NAOH. Bulk samples were prepared by centrifuging 1 mL of samples for 2 min at 13 000 rpm, removing the supernatant, and resuspending the pellet in 1 mL of 0.2 M NaOH. Both sets of samples were heated at 95 °C in a drying oven (VWR, 89511-404) for 30 min, inverting every 10 min to mix. After heating, 25 μL of prepared samples were transferred to a clear 96-well plate (VWR, 10062-900). Standards and reagents were prepared from a Pierce BCA protein assay kit (Thermo Scientific) pursuant to the protocol. A working reagent volume of 200 μL was added to each well and incubated at 37 °C for 30 min. Absorbance at 562 nm was measured using a Spectra Max M2 plate reader (Molecular Devices) and exported using Softmax Pro V5.3 (Molecular Devices). Background absorbance measurements were subtracted from samples and standards prior to determination of a standard BSA curve and sample concentration.

Data Analysis. Analysis of HPLC, integral, OD, and current data was performed using Rstudio using the following packages: ggplot2,[59] reshape2,[60] dplyr,[61] and TTR.[62]

■ ASSOCIATED CONTENT

Supporting Information

The Supporting Information is available free of charge on the ACS Publications website at DOI: 10.1021/acssynbio.8b00498.

A map of the plasmid created in this study (Figure S1), an image of a Western blot to detect PR and Bdh expression (Figure S2), 2,3-butanediol production by aerobically grown *Shewanella oneidensis* with pBBR-Bdh-PR (Figure S3), a photograph of the bioelectrochemical system (Figure S4), cell density in bioelectrochemical systems over time (Figure S5), and total protein recovery from bioelectrochemical systems at the end of experiments (Figure S6) (PDF)

■ AUTHOR INFORMATION

Corresponding Author

*E-mail: teraves2@msu.edu.

ORCID

Michaela A. TerAvest: 0000-0002-5435-3587

Author Contributions

N.M.T. designed and performed experiments, analyzed and interpreted data, and drafted the manuscript. M.A.T. designed the study, designed experiments, analyzed and interpreted data, and revised the manuscript.

Notes

The authors declare no competing financial interest.

■ ACKNOWLEDGMENTS

The authors thank Dr. Jeffrey Gralnick (University of Minnesota) for providing a plasmid containing the PR gene and Dr. N. Cecilia Martinez Gomez for helpful comments on the manuscript. This work was partially funded by NSF CAREER award 1750785. This work was also supported by the USDA National Institute of Food and Agriculture, Hatch project 1009805.

■ REFERENCES

(1) Rabaey, K., and Rozendal, R. A. (2010) Microbial Electrosynthesis — Revisiting the Electrical Route for Microbial Production. *Nat. Rev. Microbiol. 8* (10), 706−716.

(2) Rosenbaum, M. A., and Henrich, A. W. (2014) Engineering Microbial Electrocatalysis for Chemical and Fuel Production. *Curr. Opin. Biotechnol. 29* (0), 93−98.

(3) Nevin, K. P., Woodard, T. L., Franks, A. E., Summers, Z. M., and Lovley, D. R. (2010) Microbial Electrosynthesis: Feeding Microbes Electricity to Convert Carbon Dioxide and Water to Multicarbon Extracellular Organic Compounds. *mBio 1* (2), e00103−10.

(4) Nevin, K. P., Hensley, S. A., Franks, A. E., Summers, Z. M., Ou, J., Woodard, T. L., Snoeyenbos-West, O. L., and Lovley, D. R. (2011) Electrosynthesis of Organic Compounds from Carbon Dioxide Is Catalyzed by a Diversity of Acetogenic Microorganisms. *Appl. Environ. Microbiol. 77* (9), 2882−2886.

(5) Ganigué, R., Puig, S., Batlle-Vilanova, P., Balaguer, M. D., Colprim, J., Mikkelsen, M., Jørgensen, M., Krebs, F. C., Haszeldine, R.

S., Rabaey, K., et al. (2015) Microbial Electrosynthesis of Butyrate from Carbon Dioxide. *Chem. Commun. 51* (15), 3235−3238.
(6) Patil, S. A., Arends, J. B. A., Vanwonterghem, I., van Meerbergen, J., Guo, K., Tyson, G. W., and Rabaey, K. (2015) Selective Enrichment Establishes a Stable Performing Community for Microbial Electrosynthesis of Acetate from CO_2. *Environ. Sci. Technol. 49* (14), 8833−8843.
(7) Park, D. H., and Zeikus, J. G. (1999) Utilization of Electrically Reduced Neutral Red by *Actinobacillus Succinogenes*: Physiological Function of Neutral Red in Membrane-Driven Fumarate Reduction and Energy Conservation. *J. Bacteriol. 181* (8), 2403−2410.
(8) Park, D. H., Laivenieks, M., Guettler, M. V., Jain, M. K., and Zeikus, J. G. (1999) Microbial Utilization of Electrically Reduced Neutral Red as the Sole Electron Donor for Growth and Metabolite Production. *Appl. Environ. Microbiol. 65* (7), 2912−2917.
(9) Drake, H. L., Gößner, A. S., and Daniel, S. L. (2008) Old Acetogens, New Light. *Ann. N. Y. Acad. Sci. 1125*, 100−128.
(10) Müller, V. (2003) Energy Conservation in Acetogenic Bacteria. *Appl. Environ. Microbiol. 69*, 6345−6353.
(11) Ueki, T., Nevin, K. P., Woodard, T. L., and Lovley, D. R. Converting Carbon Dioxide to Butyrate with an Engineered Strain of Clostridium Ljungdahlii. *mBio* 2014, *5* (5). DOI: 10.1128/mBio.01636-14
(12) Schiel-Bengelsdorf, B., and Dürre, P. (2012) Pathway Engineering and Synthetic Biology Using Acetogens. *FEBS Lett. 586* (15), 2191−2198.
(13) Harrington, T. D., Tran, V. N., Mohamed, A., Renslow, R., Biria, S., Orfe, L., Call, D. R., and Beyenal, H. (2015) The Mechanism of Neutral Red-Mediated Microbial Electrosynthesis in *Escherichia Coli*: Menaquinone Reduction. *Bioresour. Technol. 192*, 689−695.
(14) Harrington, T. D., Mohamed, A., Tran, V. N., Biria, S., Gargouri, M., Park, J.-J., Gang, D. R., and Beyenal, H. (2015) Neutral Red-Mediated Microbial Electrosynthesis by *Escherichia coli*, *Klebsiella pneumoniae*, and *Zymomonas mobilis*. *Bioresour. Technol. 195*, 57−65.
(15) Le, Q. A. T., Kim, H. G., and Kim, Y. H. (2018) Electrochemical Synthesis of Formic Acid from CO2 Catalyzed by *Shewanella oneidensis* MR-1 Whole-Cell Biocatalyst. *Enzyme Microb. Technol. 116*, 1−5.
(16) Sakimoto, K. K., Wong, A. B., and Yang, P. (2016) Self-Photosensitization of Nonphotosynthetic Bacteria for Solar-to-Chemical Production. *Science 351* (6268), 74−77.
(17) Liu, C., Sakimoto, K. K., Colón, B. C., Silver, P. A., and Nocera, D. G. (2017) Ambient Nitrogen Reduction Cycle Using a Hybrid Inorganic−Biological System. *Proc. Natl. Acad. Sci. U. S. A. 114* (25), 6450−6455.
(18) Batlle-Vilanova, P., Puig, S., Gonzalez-Olmos, R., Balaguer, M. D., and Colprim, J. (2016) Continuous Acetate Production through Microbial Electrosynthesis from CO2with Microbial Mixed Culture. *J. Chem. Technol. Biotechnol. 91* (4), 921−927.
(19) Jourdin, L., Grieger, T., Monetti, J., Flexer, V., Freguia, S., Lu, Y., Chen, J., Romano, M., Wallace, G. G., and Keller, J. (2015) High Acetic Acid Production Rate Obtained by Microbial Electrosynthesis from Carbon Dioxide. *Environ. Sci. Technol. 49* (22), 13566−13574.
(20) Jourdin, L., Freguia, S., Flexer, V., and Keller, J. (2016) Bringing High-Rate, CO_2-Based Microbial Electrosynthesis Closer to Practical Implementation through Improved Electrode Design and Operating Conditions. *Environ. Sci. Technol. 50* (4), 1982−1989.
(21) Batlle-Vilanova, P., Ganigué, R., Ramió-Pujol, S., Bañeras, L., Jiménez, G., Hidalgo, M., Balaguer, M. D., Colprim, J., and Puig, S. (2017) Microbial Electrosynthesis of Butyrate from Carbon Dioxide: Production and Extraction. *Bioelectrochemistry 117*, 57−64.
(22) Bajracharya, S., ter Heijne, A., Dominguez Benetton, X., Vanbroekhoven, K., Buisman, C. J. N., Strik, D. P. B. T. B., and Pant, D. (2015) Carbon Dioxide Reduction by Mixed and Pure Cultures in Microbial Electrosynthesis Using an Assembly of Graphite Felt and Stainless Steel as a Cathode. *Bioresour. Technol. 195*, 14−24.
(23) Coursolle, D., and Gralnick, J. A. (2012) Reconstruction of Extracellular Respiratory Pathways for Iron(III) Reduction in *Shewanella Oneidensis* Strain MR-1. *Front. Microbiol. 3*, 56.
(24) Coursolle, D., Baron, D. B., Bond, D. R., and Gralnick, J. A. (2010) The Mtr Respiratory Pathway Is Essential for Reducing Flavins and Electrodes in *Shewanella Oneidensis*. *J. Bacteriol. 192* (2), 467−474.
(25) Clarke, T. A., Edwards, M. J., Gates, A. J., Hall, A., White, G. F., Bradley, J., Reardon, C. L., Shi, L., Beliaev, A. S., Marshall, M. J., et al. (2011) Structure of a Bacterial Cell Surface Decaheme Electron Conduit. *Proc. Natl. Acad. Sci. U. S. A. 108* (23), 9384−9389.
(26) Myers, C. R., and Myers, J. M. (2002) MtrB Is Required for Proper Incorporation of the Cytochromes OmcA and OmcB into the Outer Membrane of *Shewanella Putrefaciens* MR-1. *Appl. Environ. Microbiol. 68* (11), 5585−5594.
(27) Liu, Y., Wang, Z., Liu, J., Levar, C., Edwards, M. J., Babauta, J. T., Kennedy, D. W., Shi, Z., Beyenal, H., Bond, D. R., et al. (2014) A Trans-Outer Membrane Porin-Cytochrome Protein Complex for Extracellular Electron Transfer by *Geobacter Sulfurreducens* PCA. *Environ. Microbiol. Rep. 6* (6), 776−785.
(28) Marritt, S. J., Lowe, T. G., Bye, J., McMillan, D. G. G., Shi, L., Fredrickson, J., Zachara, J., Richardson, D. J., Cheesman, M. R., Jeuken, L. J. C., et al. (2012) A Functional Description of CymA, an Electron-Transfer Hub Supporting Anaerobic Respiratory Flexibility in *Shewanella*. *Biochem. J. 444* (3), 465−474.
(29) Fredrickson, J. K., Romine, M. F., Beliaev, A. S., Auchtung, J. M., Driscoll, M. E., Gardner, T. S., Nealson, K. H., Osterman, A. L., Pinchuk, G., Reed, J. L., et al. (2008) Towards Environmental Systems Biology of *Shewanella*. *Nat. Rev. Microbiol. 6* (8), 592−603.
(30) TerAvest, M. A., and Ajo-Franklin, C. M. (2016) Transforming Exoelectrogens for Biotechnology Using Synthetic Biology. *Biotechnol. Bioeng. 113* (4), 687−697.
(31) Schuetz, B., Schicklberger, M., Kuermann, J., Spormann, A. M., and Gescher, J. (2009) Periplasmic Electron Transfer via the C-Type Cytochromes MtrA and FccA of *Shewanella oneidensis* Mr-1. *Appl. Environ. Microbiol. 75*, 7789.
(32) Ross, D. E., Ruebush, S. S., Brantley, S. L., Hartshorne, R. S., Clarke, T. A., Richardson, D. J., and Tien, M. (2007) Characterization of Protein-Protein Interactions Involved in Iron Reduction by *Shewanella oneidensis* MR-1. *Appl. Environ. Microbiol. 73*, 5797.
(33) Beliaev, A. S., Saffarini, D. A., McLaughlin, J. L., and Hunnicutt, D. (2001) MtrC, an Outer Membrane Decahaem c Cytochrome Required for Metal Reduction in *Shewanella putrefaciens* MR-1. *Mol. Microbiol. 39*, 722.
(34) Gralnick, J. A., and Newman, D. K. (2007) Extracellular Respiration. *Mol. Microbiol. 65* (1), 1−11.
(35) Ross, D. E., Flynn, J. M., Baron, D. B., Gralnick, J. A., and Bond, D. R. (2011) Towards Electrosynthesis in *Shewanella*: Energetics of Reversing the Mtr Pathway for Reductive Metabolism. *PLoS One 6* (2), No. e16649.
(36) Rowe, A. R., Rajeev, P., Jain, A., Pirbadian, S., Okamoto, A., Gralnick, J. A., El-Naggar, M. Y., and Nealson, K. H. Tracking Electron Uptake from a Cathode into *Shewanella* Cells: Implications for Energy Acquisition from Solid-Substrate Electron Donors. *mBio* 2018, *9* (1). DOI: 10.1128/mBio.02203-17
(37) Pinchuk, G. E., Hill, E. A., Geydebrekht, O. V., De Ingeniis, J., Zhang, X., Osterman, A., Scott, J. H., Reed, S. B., Romine, M. F., Konopka, A. E., et al. (2010) Constraint-Based Model of *Shewanella oneidensis* MR-1 Metabolism: A Tool for Data Analysis and Hypothesis Generation. *PLoS Comput. Biol. 6* (6), No. e1000822.
(38) Spero, M. A., Aylward, F. O., Currie, C. R., and Donohue, T. J. (2015) Phylogenomic Analysis and Predicted Physiological Role of the Proton-Translocating NADH:Quinone Oxidoreductase (Complex I) across Bacteria. *mBio 6* (2), e00389.
(39) Spero, M. A., Brickner, J. R., Mollet, J. T., Pisithkul, T., Amador-Noguez, D., and Donohue, T. J. (2016) Different Functions of Phylogenetically Distinct Bacterial Complex I Isozymes. *J. Bacteriol. 198* (8), 1268−1280.
(40) Salis, H. M. (2011) The Ribosome Binding Site Calculator. *Methods Enzymol. 498*, 19−42.
(41) Johnson, E. T., Baron, D. B., Naranjo, B., Bond, D. R., Schmidt-Dannert, C., and Gralnick, J. A. (2010) Enhancement of Survival and

DOI: 10.1021/acssynbio.8b00498
ACS Synth. Biol. 2019, 8, 1590−1600

Electricity Production in an Engineered Bacterium by Light-Driven Proton Pumping. *Appl. Environ. Microbiol. 76* (13), 4123−4129.
(42) Hunt, K. A., Flynn, J. M., Naranjo, B., Shikhare, I. D., and Gralnick, J. A. (2010) Substrate-Level Phosphorylation Is the Primary Source of Energy Conservation during Anaerobic Respiration of *Shewanella Oneidensis* Strain MR-1. *J. Bacteriol. 192* (13), 3345−3351.
(43) Marshall, M. J., Plymale, A. E., Kennedy, D. W., Shi, L., Wang, Z., Reed, S. B., Dohnalkova, A. C., Simonson, C. J., Liu, C., Saffarini, D. A., et al. (2008) Hydrogenase- and Outer Membrane *c*-Type Cytochrome-Facilitated Reduction of Technetium(VII) by *Shewanella Oneidensis* MR-1. *Environ. Microbiol. 10* (1), 125−136.
(44) Meshulam-Simon, G., Behrens, S., Choo, A. D., and Spormann, A. M. (2007) Hydrogen Metabolism in *Shewanella oneidensis* MR-1. *Appl. Environ. Microbiol. 73* (4), 1153−1165.
(45) Kreuzer, H. W., Hill, E. A., Moran, J. J., Bartholomew, R. A., Yang, H., and Hegg, E. L. (2014) Contributions of the [NiFe]- and [FeFe]-Hydrogenase to H_2 Production in *Shewanella Oneidensis* MR-1 as Revealed by Isotope Ratio Analysis of Evolved H_2. *FEMS Microbiol. Lett. 352* (1), 18−24.
(46) Pinchuk, G. E., Geydebrekht, O. V., Hill, E. A., Reed, J. L., Konopka, A. E., Beliaev, A. S., and Fredrickson, J. K. (2011) Pyruvate and Lactate Metabolism by *Shewanella Oneidensis* MR-1 under Fermentation, Oxygen Limitation, and Fumarate Respiration Conditions. *Appl. Environ. Microbiol. 77* (23), 8234−8240.
(47) Brutinel, E. D., and Gralnick, J. A. (2012) Anomalies of the Anaerobic Tricarboxylic Acid Cycle in *Shewanella Oneidensis* Revealed by Tn-Seq. *Mol. Microbiol. 86* (2), 273−283.
(48) Jensen, H. M., Albers, A. E., Malley, K. R., Londer, Y. Y., Cohen, B. E., Helms, B. A., Weigele, P., Groves, J. T., and Ajo-Franklin, C. M. (2010) Engineering of a Synthetic Electron Conduit in Living Cells. *Proc. Natl. Acad. Sci. U. S. A. 107* (45), 19213−19218.
(49) Rowe, A. R., Rajeev, P., Jain, A., Pirbadian, S., Okamoto, A., Gralnick, J. A., El-Naggar, M. Y., and Nealson, K. Tracking Electron Uptake from a Cathode into *Shewanella* Cells: Implications for Generating Maintenance Energy from Solid Substrates. *mBio* 2018. DOI: 10.1128/mBio.02203-17
(50) Duhl, K. L., Tefft, N. M., and TerAvest, M. A. *Shewanella oneidensis* MR-1 Utilizes Both Sodium- and Proton-Pumping NADH Dehydrogenases during Aerobic Growth. *Appl. Environ. Microbiol.* 2018, *84* (12). DOI: 10.1128/AEM.00415-18
(51) Covington, E. D., Gelbmann, C. B., Kotloski, N. J., and Gralnick, J. A. (2010) An Essential Role for UshA in Processing of Extracellular Flavin Electron Shuttles by Shewanella Oneidensis. *Mol. Microbiol. 78* (2), 519−532.
(52) Kotloski, N. J., and Gralnick, J. A. (2013) Flavin Electron Shuttles Dominate Extracellular Electron Transfer by *Shewanella Oneidensis*. *mBio 4* (1), e00553.
(53) Brutinel, E., and Gralnick, J. (2012) Shuttling Happens: Soluble Flavin Mediators of Extracellular Electron Transfer in *Shewanella*. *Appl. Microbiol. Biotechnol. 93* (1), 41−48.
(54) Okamoto, A., Hashimoto, K., and Nealson, K. H. (2014) Flavin Redox Bifurcation as a Mechanism for Controlling the Direction of Electron Flow during Extracellular Electron Transfer. *Angew. Chem., Int. Ed. 53* (41), 10988−10991.
(55) Hemmerich, P., Knappe, W., Kramer, H. E. A., and Traber, R. (1980) Distinction of 2e− and 1e− Reduction Modes of the Flavin Chromophore as Studied by Flash Photolysis. *Eur. J. Biochem. 104* (2), 511−520.
(56) Einhauer, A., and Jungbauer, A. (2001) The FLAG™ Peptide, a Versatile Fusion Tag for the Purification of Recombinant Proteins. *J. Biochem. Biophys. Methods 49* (1−3), 455−465.
(57) De Lorenzo, V., Herrero, M., Jakubzik, U., and Timmis, K. N. (1990) Mini-Tn5 Transposoon Derivatives for Insertion Mutagenesis, Promoter Probing, and Chromosomal Insertion of Cloned DNA in Gram-Negative Eubacteria. *J. Bacteriol. 172* (11), 6568−6572.
(58) Fuhrman, J. A., Schwalbach, M. S., and Stingl, U. (2008) Proteorhodopsins: An Array of Physiological Roles? *Nat. Rev. Microbiol. 6* (6), 488−494.
(59) Wickham, H. *Ggplot2 Elegant Graphics for Data Analysis*; Springer: 2009; Vol. *35*.
(60) Wickham, H. (2007) Reshaping Data with the Reshape Package. *J. Stat. Softw. 21* (12), 1−20.
(61) Wickham, H., and Francois, R. *Dplyr: A Grammar of Data Manipulation*, R Packag. version 0.4.2.; R Studio: 2015, 3.
(62) Ulrich, J. *TTR: Technical Trading Rules*, R Packag. version 0.23-2; 2017.
(63) Myers, C. R., and Nealson, K. H. (1988) Bacterial Manganese Reduction and Growth with Manganese Oxide as the Sole Electron Acceptor. *Science 240*, 1319−1321.
(64) Meshulam-Simon, G., Behrens, S., Choo, A. D., and Spormann, A. M. (2007) Hydrogen Metabolism in Shewanella Oneidensis MR-1. *Appl. Environ. Microbiol. 73* (4), 1153−1165.
(65) Yazynin, S. A., Deyev, S. M., Jucovič, M., and Hartley, R. W. (1996) A Plasmid Vector with Positive Selection and Directional Cloning Based on a Conditionally Lethal Gene. *Gene 169* (1), 131−132.
(66) Beja, O., Aravind, L., Koonin, E. V., Suzuki, M. T., Hadd, A., Nguyen, L. P., Jovanovich, S. B., Gates, C. M., Feldman, R. A., Spudich, J. L., et al. (2000) Bacterial Rhodopsin: Evidence for a New Type of Phototrophy in the Sea. *Science 289*, 1902−1906.

DOI: 10.1021/acssynbio.8b00498
ACS Synth. Biol. 2019, 8, 1590−1600